JOURNAL OF THE AMERICAN COLLEGE OF CARDIOLOGY VOL. 77, NO. 7, 2021

Subclinical Atherosclerosis and Brain Metabolism in Middle-Aged Individuals

The PESA Study

Marta Cortes-Canteli, PhD,[a,*] Juan Domingo Gispert, PhD,[b,c,d,e,*] Gemma Salvadó, MSc,[b,c] Raquel Toribio-Fernandez, PhD,[a] Catarina Tristão-Pereira, MSc,[a] Carles Falcon, PhD,[b,d] Belen Oliva, MSc,[a] Jose Mendiguren, MD,[f] Leticia Fernandez-Friera, MD, PhD,[a,g,h] Javier Sanz, MD,[a,i] Jose M. Garcia-Ruiz, MD,[a,h,j] Antonio Fernandez-Ortiz, MD, PhD,[a,h,k] Javier Sanchez-Gonzalez, PhD,[l] Borja Ibanez, MD, PhD,[a,h,m] José Luis Molinuevo, MD, PhD,[b,c,e,n,†] Valentin Fuster, MD, PhD[a,i,†]

ABSTRACT

BACKGROUND Atherosclerosis has been linked to cognitive decline in late life; however, the impact of cardiovascular risk factors (CVRFs) and subclinical atherosclerosis on brain metabolism at earlier stages remains unexplored.

OBJECTIVES This study sought to determine the association between brain metabolism, subclinical atherosclerosis, and CVRFs in middle-aged asymptomatic individuals.

METHODS This study included 547 asymptomatic middle-aged participants (50 ± 4 years, 82% men) from the PESA (Progression of Early Subclinical Atherosclerosis) study with evidence of subclinical atherosclerosis. Participants underwent ^{18}F-fluorodeoxyglucose (FDG)-positron emission tomography. Global brain FDG uptake and voxel-wise analyses were used to evaluate the associations of cerebral metabolism with CVRFs and atherosclerotic plaque burden in carotids and femorals assessed by 3-dimensional vascular ultrasound.

RESULTS Global FDG uptake showed an inverse correlation with 30-year Framingham Risk Score (FRS) ($\beta = -0.15$, $p < 0.001$). This association was mainly driven by the presence of hypertension ($d = 0.36$, $p < 0.001$). Carotid plaque burden was inversely associated with global brain FDG uptake ($\beta = -0.16$, $p < 0.001$), even after adjusting for 30-year FRS. Voxel-wise approaches revealed that the brain areas most strongly affected by hypometabolism in association with 30-year FRS, hypertension, and carotid plaque burden were parietotemporal regions (angular, supramarginal, and inferior/middle temporal gyri) and the cingulate gyrus.

CONCLUSIONS In asymptomatic middle-aged individuals, cardiovascular risk is associated with brain hypometabolism, with hypertension being the modifiable CVRF showing the strongest association. Subclinical carotid plaque burden is also linked to reduced brain metabolism independently of CVRFs. Cerebral areas showing hypometabolism include those known to be affected in dementia. These data reinforce the need to control CVRFs early in life in order to potentially reduce the brain's midlife vulnerability to future cognitive dysfunction. (J Am Coll Cardiol 2021;77:888–98)

From the [a]Centro Nacional de Investigaciones Cardiovasculares (CNIC), Madrid, Spain; [b]Barcelonaβeta Brain Research Center (BBRC), Pasqual Maragall Foundation, Barcelona, Spain; [c]IMIM (Hospital del Mar Medical Research Institute), Barcelona, Spain; [d]Centro de Investigación Biomédica en Red (CIBER) de Bioingeniería, Biomateriales y Nanomedicina, Madrid, Spain; [e]Universitat Pompeu Fabra, Barcelona, Spain; [f]Banco de Santander, Madrid, Spain; [g]HM Hospitales-Centro Integral de Enfermedades Cardiovasculares, Universidad San Pablo-CEU, Madrid, Spain; [h]CIBER de enfermedades Cardiovasculares, Madrid, Spain; [i]Icahn School of Medicine at Mount Sinai, New York, New York, USA; [j]Hospital Universitario Central de Oviedo, Asturias, Spain; [k]Hospital Clínico San Carlos, Instituto de Investigación Sanitaria San Carlos, Universidad Complutense, Madrid, Spain; [l]Philips Healthcare Iberia, Spain; [m]Instituto de Investigación Sanitaria-Fundación Jiménez Díaz, Madrid, Spain; and [n]CIBER Fragilidad y Envejecimiento Saludable, Madrid, Spain. *Drs. Cortes-Canteli and Gispert are joint first authors. †Drs. Molinuevo and Fuster are joint corresponding authors. Costantino Iadecola, MD, served as Guest Associate Editor for this paper. Athena Poppas, MD, served as Guest Editor-in-Chief for this paper.

The authors attest they are in compliance with human studies committees and animal welfare regulations of the authors' institutions and Food and Drug Administration guidelines, including patient consent where appropriate. For more information, visit the Author Center.

Manuscript received November 9, 2020; revised manuscript received December 15, 2020, accepted December 15, 2020.

Listen to this manuscript's audio summary by Editor-in-Chief Dr. Valentin Fuster on JACC.org.

ISSN 0735-1097 https://doi.org/10.1016/j.jacc.2020.12.027

Atherosclerosis, the underlying cause of most cardiovascular diseases (CVDs) and the leading cause of death and morbidity worldwide (1), is a long-lasting process beginning in the early decades of life. The identification of atherosclerosis in its subclinical stages is an emerging strategy for improved primary prevention (2–4), and current clinical practice guidelines recommend screening for subclinical atherosclerosis in different vascular territories and its inclusion as a risk modifier with implications for intervention (5,6).

Dementia is among the top causes of disability and death worldwide and is one of the global challenges of the century (7). Dementia is characterized by a progressive deterioration of cognitive ability and includes a number of different disorders, with Alzheimer's disease (AD) being the most common followed by vascular dementia. Fifty million people live with dementia worldwide, and, due to population aging, this figure is predicted to reach 150 million people by 2050 if there is no progress in prevention, intervention, and care (7).

The presence of atherosclerosis has been linked to cognitive impairment at advanced stages (8,9). Intracranial atherosclerotic disease in elderly persons is associated with an increased prevalence of mild cognitive impairment and dementia (10), and cerebral atherosclerosis and arteriolosclerosis are linked to lower scores in most cognitive domains and to higher odds of AD in the very old (11). The link between atherosclerosis and cognitive decline extends to extracranial vessels, with the presence of carotid and femoral atherosclerosis showing an association with vascular dementia and AD in the elderly population (12,13). Shared risk factors for atherosclerosis and dementia include hypertension, diabetes, cholesterol levels, sedentary lifestyle, and smoking (14). Previous studies reported that elderly individuals with some of these cardiovascular risk factors (CVRFs) show decreased brain glucose uptake (15–17). Despite this evidence, little is known about how atherosclerosis and cognitive decline influence each other and whether they share a common trajectory during their long asymptomatic stages (18,19). Understanding the extent to which CVRFs influence the brain's vulnerability early in the course of atherosclerosis (during midlife) may help to refine preventive strategies and reduce the incidence of dementia in late life.

The PESA (Progression of Early Subclinical Atherosclerosis; NCT01410318) study is a prospective cohort study of more than 4,000 asymptomatic middle-aged participants exhaustively evaluated for the presence and extent of subclinical atherosclerosis (20,21). A subcohort of the PESA population underwent whole-body ^{18}F-fluorodeoxyglucose (FDG)-positron emission tomography (PET) imaging to study metabolic activity associated with arterial atherosclerosis (22). Using images from this analysis, which included brain imaging, we studied the association of cerebral metabolism (FDG uptake) with CVRFs and atherosclerotic plaque burden.

SEE PAGE 899

ABBREVIATIONS AND ACRONYMS

AD = Alzheimer's disease

CVD = cardiovascular disease

CVRF = cardiovascular risk factor

FRS = Framingham Risk Score

FDG = fluorodeoxyglucose

PCA = principal component analysis

PET = positron emission tomography

METHODS

STUDY DESIGN AND POPULATION. PESA is a prospective cohort study of 4,184 asymptomatic middle-aged (40 to 54 years) employees at the Banco Santander headquarters in Madrid, Spain, that investigates the prevalence, progression, and determinants of subclinical atherosclerosis. The study design and atherosclerosis prevalence at baseline have been reported previously (20,21). The study excluded individuals with previous CVD, cancer, or any other disease expected to shorten life span or influence protocol adherence. Baseline CVRF data and subclinical atherosclerosis measurements (2-dimensional/3-dimensional [3D] vascular ultrasound and noncontrast computed tomography for coronary artery calcification assessment) were performed from June 2010 to March 2014. CVRFs were determined from interview questionnaires and blood samples as follows: diabetes mellitus as fasting plasma glucose ≥126 mg/dl or treatment with insulin or oral hypoglycemic medication; arterial hypertension as systolic blood pressure ≥140 mm Hg, diastolic blood pressure ≥90 mm Hg, or use of antihypertensive medication; dyslipidemia as total cholesterol ≥240 mg/dl, low-density lipoprotein cholesterol ≥160 mg/dl, high-density lipoprotein cholesterol <40 mg/dl, or use of lipid-lowering drugs; and smoking as current smoking status and a lifetime consumption of >100 cigarettes. Cardiovascular risk was estimated as the Framingham Heart Study CVD risk at 30 years (30-year Framingham risk score [FRS]) (21,23). Atherosclerotic plaque volume was quantified using the standardized 6-cm acquisition performed with 3D vascular ultrasound (24,25). Carotid and femoral plaque burden were defined as the sum of plaque volumes in the right/left carotid and right/left femoral arteries, respectively, and the total plaque burden as the sum of carotid and femoral plaque burden.

A subcohort of PESA participants (N = 946) showing evidence of atherosclerosis in baseline examinations underwent vascular FDG-PET (22). The inclusion criteria were the presence of coronary artery calcification (score ≥ 1) or being in the highest

FIGURE 1 The Study Flow

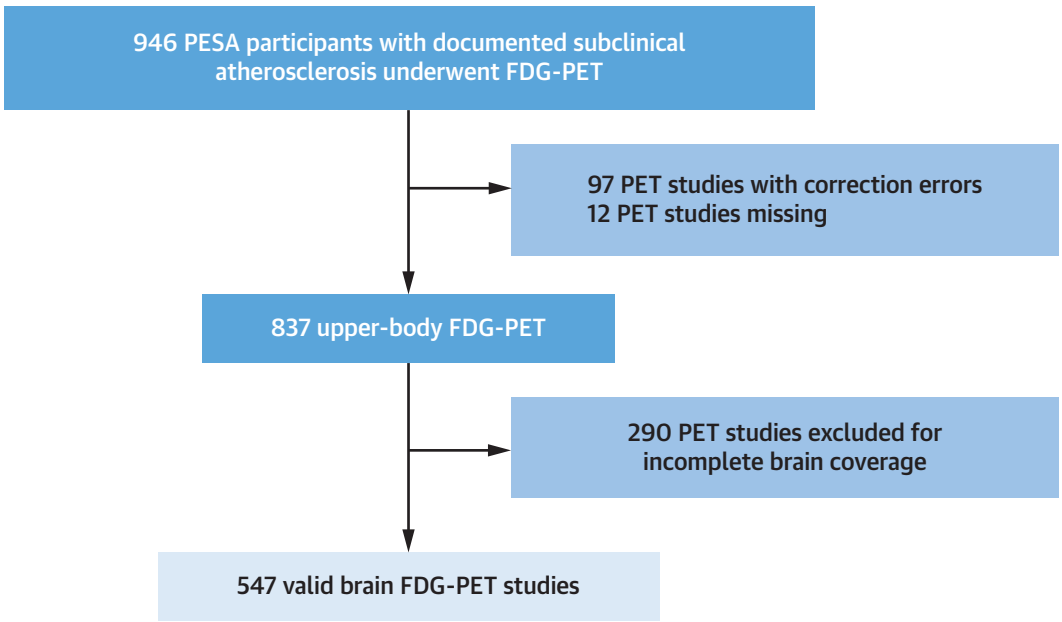

A total of 946 PESA (Progression of Early Subclinical Atherosclerosis) participants with documented subclinical atherosclerosis underwent full-body ^{18}F-fluorodeoxyglucose (FDG)-positron emission tomography (PET). Of these, missing studies and those with errors were removed, leaving a total of 837 upper-body FDG-PET studies available for analysis. After image processing and careful examination, 290 cases were excluded for incomplete brain coverage, yielding 547 valid FDG-PET brain studies for analysis.

plaque thickness tertile. FDG-PET image acquisition was performed from February 2013 to January 2015.

The PESA study was approved by the ethics committee of the Instituto de Salud Carlos III in Madrid, and all participants provided informed consent for all clinical evaluations before enrollment.

PET ACQUISITION. The acquisition protocol has been described previously (22). Briefly, all participants received a target dose of 270 to 300 MBq FDG and underwent a carotid PET scan 120 min after radiotracer injection. The associated radiation exposure was calculated according to International Commission on Radiological Protection Task Group on Radiation Dose criteria. Upper-body craniocaudal PET scans in 5 bed positions (3 min/bed) were acquired with a hybrid PET/magnetic resonance Philips Ingenuity system (Philips Healthcare, Cleveland, Ohio) (22). Data were reconstructed in 3D mode using a blob-based, list-mode iterative algorithm with time-of-flight information and were corrected for attenuation using magnetic resonance imaging attenuation maps. Reconstructed images had a transverse field of view of 576 mm and a voxel size of $4 \times 4 \times 4$ mm^3. All images were reviewed by expert technologists, radiologists, or nuclear medicine specialists.

CEREBRAL FDG-PET ANALYSIS. Complete upper-body FDG-PET scan data were available from 837 baseline studies. Images were cropped to retain brain regions in the field of view and were spatially normalized to a sample-specific template in the standard space of the Montreal Neurological Institute (26) using the algorithm in the SPM12 package. Normalized image quality was assessed with the CAT12 toolbox for SPM12. Images not achieving a sample homogeneity of $r > 0.95$ were discarded, and the procedure was iterated until all images survived this quality indicator. Finally, all images were inspected visually. At the end of this process, 547 valid brain FDG-PET studies were available for subsequent image quantification.

FDG uptake in the scans was normalized to that of the cerebellar vermis, which has been identified as the most suitable reference region because of its low intraindividual metabolic glucose rate variability (27). The resulting parametric standard uptake value ratio images were smoothed with a Gaussian kernel of 8 mm full width at half maximum.

STATISTICAL ANALYSIS. Two main analyses were performed: a hypothesis-driven global whole-brain analysis and an unbiased voxel-wise approach. The

TABLE 1 Demographics and Clinical Characteristics of the Study Sample (N = 547)

Age, yrs	50.3 ± 4.4
Men	451 (82.5)
Smoking	146 (27.1)
Hypertension	108 (19.7)
Diabetes	25 (4.6)
Systolic blood pressure, mm Hg	121.6 ± 12.3
Diastolic blood pressure, mm Hg	75.8 ± 8.7
Body mass index, kg/m^2	27.3 ± 3.5
Total cholesterol, mg/dl	209.0 ± 34.3
High-density lipoprotein cholesterol, mg/dl	45.5 ± 11.4
Dyslipidemia	328 (60.0)
Total plaque burden, mm^3	79.6 (13.7–183.0)
Carotid plaque burden, mm^3	3.7 (0–35.6)
Femoral plaque burden, mm^3	46.2 (0–143.2)
30-yr Framingham Risk Score, %	24.2 (16.3–33.0)

Values are mean ± SD, n (%), or median (interquartile range). All values are calculated with data from all 547 study participants, except for smoking and plaque burden, where data were available for 538 and 505 participants, respectively.

aim of the whole-brain analysis was to determine whether global cerebral metabolism was influenced by 30-year FRS, individual CVRFs, or the presence of 3D vascular ultrasound-quantified subclinical atherosclerosis. For this analysis, we calculated the volume-weighted mean FDG uptake in the gray matter (excluding the cerebellum). The voxel-wise approach compared FDG uptake in all brain images voxel by voxel and was aimed at identifying regional patterns of cerebral glucose consumption associated with 30-year FRS, the presence of individual CVRFs, or 3D vascular ultrasound-quantified subclinical atherosclerosis.

For both approaches, similar statistical models were constructed, with the dependent variables being FDG uptake in the whole brain or at the voxel level. Covariates in both approaches were age, sex, and blood glucose levels at the time of the PET scan. Variables of interest such as plaque burden (mm^3) and 30-year FRS were included in independent models. Because of their non-normal distribution, plaque burden variables were log transformed. Moreover, an independent model was constructed including all CVRFs in the 30-year FRS as variables of interest (with glucose levels at the time of the PET as the only covariate). Because the CVRFs included in the 30-year FRS are highly correlated, we performed a principal component analysis (PCA) to decipher the independent association of each CVRF with FDG uptake. Thus, the PCA allowed us to avoid problems of collinearity, which could lead to misinterpretation (Supplemental Figure 1). The PCA was performed with the varimax rotation function in the Statistical Package for the Social Sciences v24 (SPSS Inc., Chicago, Illinois). We opted for a model with 7 output variables because total cholesterol and high-density lipoprotein cholesterol values were so highly correlated that it was impossible to disentangle them. Therefore, the final model included the principal components of age, sex, systolic blood pressure, smoking, hypertension, diabetes, and dyslipidemia (total and high-density lipoprotein cholesterol as a single variable). For the multiple regression analysis of whole-brain models, p values are accompanied by the standardized regression coefficient (β) for continuous variables and by Cohen's d for categoric variables. Voxel-wise analyses were conducted in SPM12. Brain regions showing significant effects were identified using the threshold-free cluster-enhancement method (28) implemented in SPM12. A family-wise error approach ($p < 0.05$) was used to correct for multiple comparisons.

RESULTS

DEMOGRAPHIC DATA FOR THE BRAIN FDG-PET PESA SUBPOPULATION. A total of 946 FDG-PET studies were acquired in the PESA population at baseline. Because of technical difficulties, 109 cases had to be discarded, thus leaving 837 FDG-PET studies available for analysis. Although cerebral FDG-PET was not a primary objective of the PESA study, full brain coverage was obtained in 547 FDG-PET studies, which formed the final sample (**Figure 1**). Within this participant sample, the mean age at the time of FDG-PET acquisition was 50.3 ± 4.4 years, 451 (82.5%) were men, and all were Caucasians and professionally active. The most prevalent risk factor was dyslipidemia (60%) followed by smoking (27.1%), hypertension (19.7%), and diabetes (4.6%). The median 30-year FRS was 24.2% (interquartile range: 16.3 to 33.0). The total plaque burden (carotids plus femorals) was 79.6 mm^3 (interquartile range: 13.7 to 183.0 mm^3). Carotid plaque burden was 3.7 mm^3 (interquartile range: 0 to 35.6 mm^3), and the femoral plaque burden was 46.2 mm^3 (interquartile range: 0 to 143.2 mm^3) (**Table 1**).

CVRFs AND BRAIN METABOLISM. We first analyzed whether there was an association between CVRFs and global cerebral FDG uptake by using validated risk equations. Because the PESA population has a low cardiovascular risk, mainly because of its relatively young age, we assessed cardiovascular risk using the 30-year FRS scale (23). Global brain FDG uptake was inversely associated with the 30-year FRS ($\beta = -0.15$, $p < 0.001$) (**Figure 2A**). Next, we used a hypothesis-free voxel-wise approach to identify which specific

FIGURE 2 CVRFs Are Associated With Decreased Brain FDG Uptake in Middle-Aged Asymptomatic Individuals

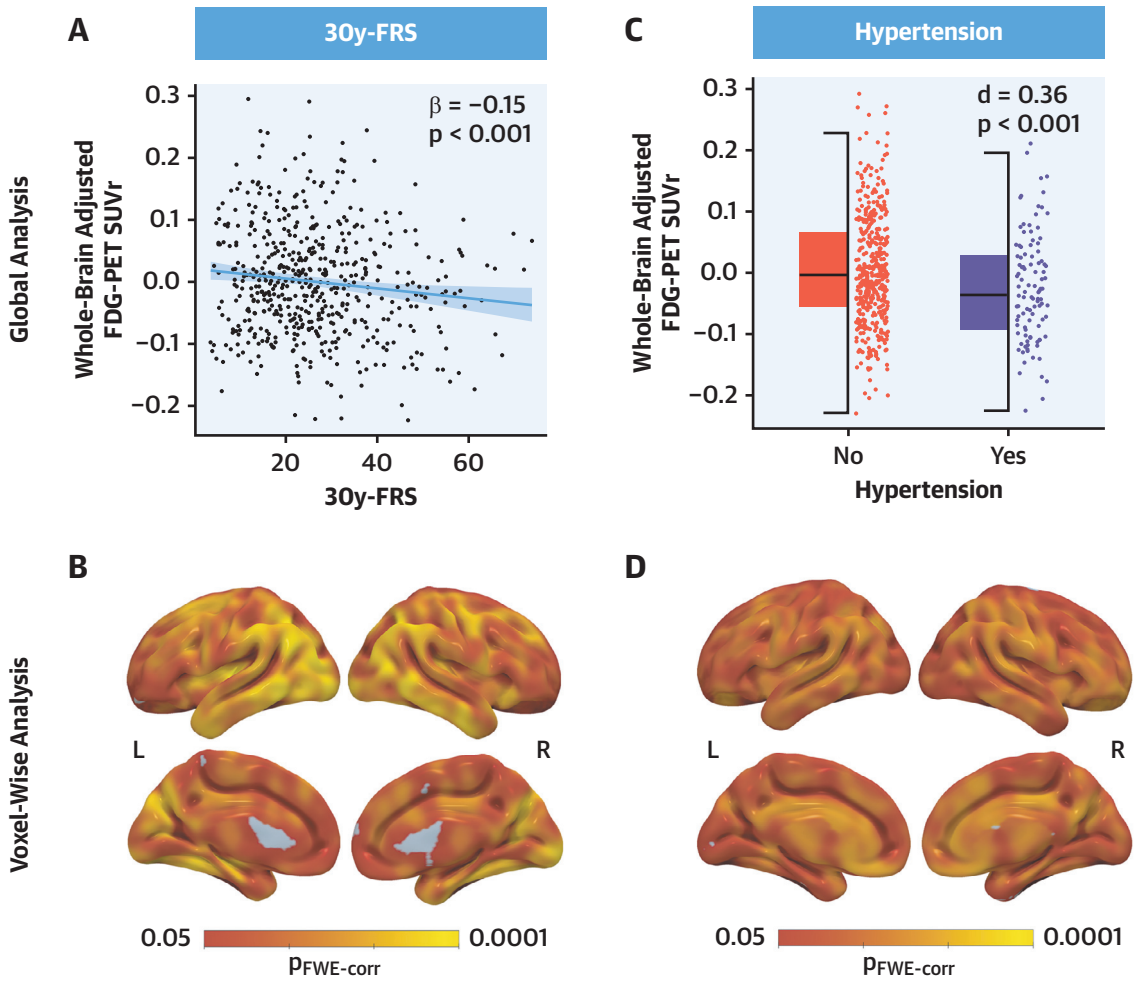

(A) A **scatterplot** showing the correlation between whole-brain adjusted FDG-PET standard uptake value ratio (SUVr) and 30-year Framingham Risk Score (30y-FRS) ($\beta = -0.15$, $p < 0.001$), indicating a significant association between global cerebral hypometabolism and high 30y-FRS. **(B)** Three-dimensional brain statistical parametric maps highlighting the areas in which high 30y-FRS is associated with reduced FDG uptake. The correlation analysis for **A** and **B** included age, sex, and baseline plasma glucose. **(C)** A **boxplot** showing significantly lower global brain FDG uptake in the hypertensive subpopulation than in individuals without hypertension ($d = 0.36$, $p < 0.001$). **(D)** Three-dimensional brain statistical parametric maps with principal component analysis (PCA) indicating an association between the presence of hypertension and hypometabolism in different brain areas, independent of other cardiovascular risk factors. The correlation analysis for **C** and **D** included baseline plasma glucose as a covariate together with the following PCA factors: age, sex, systolic blood pressure, total cholesterol, high-density lipoprotein cholesterol, smoking, hypertension, and diabetes. The line in **A** represents the regression line, and the shading around it corresponds to the 95% confidence interval. The **horizontal line** within the boxes in **C** represents the median, and the top and bottom edges of the boxes correspond to the 75th (P75) and 25th (P25) percentiles, respectively. The **vertical lines** that extend from the top and bottom of the boxes indicate the maximum (P75 + 1.5 * interquartile range [IQR]) and the minimum (P25 − 1.5 * IQR) values, respectively. **Color bars** in **B** and **D** represent the magnitude of the voxel significance corrected for multiple comparisons ($P_{FWE\text{-}corr}$). L = left; R = right; other abbreviations as in Figure 1.

cerebral regions showed decreased FDG uptake. Family-wise error-corrected statistical parametric maps showed that a high 30-year FRS correlated with reduced FDG uptake predominantly in areas of the parietotemporal region, specifically the angular and middle/inferior temporal gyri (Figure 2B, Table 2, Supplemental Figure 2).

We next conducted a PCA to decipher which of the CVRFs included in the 30-year FRS was independently associated with brain FDG uptake. The

TABLE 2 Hypometabolic Brain Regions Associated With High 30y-FRS, the Presence of Hypertension, and Carotid Plaque Burden

	High 30y-FRS		Hypertension		High Carotid Plaque Burden		High Carotid Plaque Burden Adjusted for Total Plaque Burden		High Carotid Plaque Burden Adjusted for 30y-FRS	
Brain Region	x; y; z	pFWE	x; y; z	pFWE	x; y; z	pFWE	x; y; z	pFWE	x; y; z	pFWE
R angular gyrus	36; −68; 48	<0.001			40; −70; 46	<0.001	56; −56; 46	0.003	40; −72; 44	<0.001
L angular gyrus	−52; −70; 24	<0.001	−26; −72; 38	0.001						
R anterior cingulate gyrus			0; 38; −6	0.001						
L anterior cingulate gyrus			−2; 36; −10	0.001						
R middle cingulate gyrus			6; −20; 40	0.001						
R posterior cingulate gyrus			8; −30; 38	0.001					12; −34; 46	0.001
L posterior cingulate gyrus			0; −32; 46	0.001	−2; −38; 46	<0.001			−2; −38; 46	<0.001
R supramarginal gyrus					56; −42; 50	<0.001	56; −44; 50	0.002	56; −42; 50	<0.001
R superior parietal lobule					38; −40; 48	<0.001	38; −40; 44	0.003	40; −56; 60	<0.001
R postcentral gyrus					48; −26; 64	<0.001				
R precuneus									4; −60; 68	0.001
R inferior temporal gyrus	62; −60; −12	<0.001								
L inferior temporal gyrus	−58; −56; −16	<0.001								
R middle temporal gyrus	64; −54; −2	<0.001					54; −66; 12	0.003		
R cuneus			14; −68; 26	0.001						
L cuneus							−10; −78; 30	0.003		

The table lists some of the most significant hypometabolic brain regions in each of the voxel-wise analyses shown in Figures 2 and 3. Hypometabolic locations within the indicated brain regions are given as anatomic atlas Montreal Neurological Institute coordinates (x; y; z, mm).

30y-FRS = 30-year Framingham Risk Score; pFWE = p values obtained after family-wise error correction.

modifiable CVRF showing the strongest association with global cerebral hypometabolism was the presence of hypertension, with a moderate but highly significant effect size ($d = 0.36$, $p < 0.001$) (**Figure 2C**, Supplemental Table 1). Statistical parametric mapping showed that the most affected regions were the cingulate gyri within the limbic system, together with specific areas of the parietal lobe (angular gyrus) and occipital lobe (cuneus) (**Figure 2D, Table 2**, Supplemental Figure 3). As expected, the voxel-wise analysis also highlighted hypometabolic brain regions in older participants (Supplemental Figures 4A and 4B, Supplemental Table 2) and men (Supplemental Figures 4C and 4D, Supplemental Table 2). Furthermore, systolic blood pressure was also identified as a contributing factor to reduced brain FDG uptake, with a different spatial distribution including regions such as the parahippocampal and inferior temporal gyri (Supplemental Figures 4E and 4F, Supplemental Table 2).

SUBCLINICAL ATHEROSCLEROSIS BURDEN AND BRAIN METABOLISM. We next analyzed the association between the burden of subclinical atherosclerosis and brain metabolism. Global brain FDG uptake showed no significant association with total atheroma plaque burden ($\beta = -0.04$, $p = 0.318$) (Supplemental Figure 5). However, the voxel-wise analysis highlighted specific hypometabolic brain regions significantly associated with total plaque burden (Supplemental Figure 6). Because the total plaque burden in this study includes plaque volume in the femoral and carotid arteries, we next evaluated the separate influence of each of these territories on brain metabolism. The femoral plaque burden showed no correlation with brain FDG uptake in our cohort ($\beta = -0.05$, $p = 0.293$) (Supplemental Figure 7). On the other hand, carotid plaque burden showed a significant inverse correlation with global brain metabolism ($\beta = -0.16$, $p < 0.001$, **Figure 3A**). The regional analysis revealed that some of the most significantly hypometabolic regions associated with carotid plaque were the posterior cingulate gyrus and parietal regions such as the angular and supramarginal gyri (**Figure 3B, Table 2**, Supplemental Figure 8). The association between a high carotid plaque burden and reduced brain FDG uptake remained significant after adjusting for the total plaque burden, indicating that the association was independent of the presence of atherosclerosis in the femoral arteries (**Figures 3C and 3D**). Moreover, the inverse association between carotid plaque burden and cerebral FDG uptake also remained significant after adjusting for 30-year FRS, both when analyzing the brain globally ($\beta = -0.13$, $p = 0.002$, **Figure 3E**) and when using the voxel-wise approach (**Figure 3F, Table 2**, Supplemental Figure 9).

DISCUSSION

The main findings of this study are that in middle-aged asymptomatic individuals: 1) the CVD risk

FIGURE 3 Subclinical Carotid Plaque Burden Is Associated With Reduced Brain FDG Uptake in Middle-Aged Asymptomatic Individuals

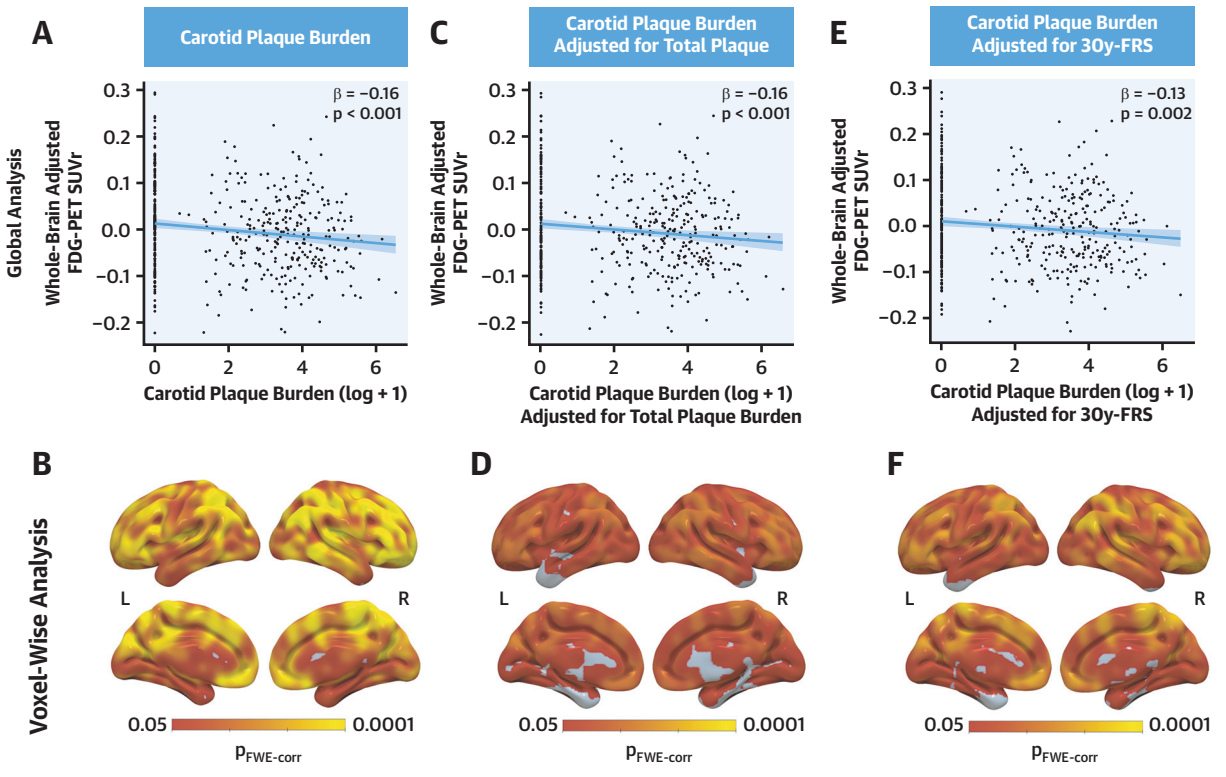

(A, C, and E) Scatterplots showing inverse correlations between whole-brain adjusted FDG-PET SUVr and carotid plaque burden, carotid plaque adjusted for total plaque burden, and carotid plaque burden adjusted for 30y-FRS. **(B)** Three-dimensional brain statistical parametric maps highlighting the hypometabolic brain areas with subclinical disease burden in the carotid arteries. This correlation is maintained after adjusting for **(D)** log-transformed total plaque volume or **(F)** 30y-FRS. All correlation analyses included age, sex, and baseline plasma glucose as covariates. The correlation analysis for **C, D, E,** and **F** additionally included log-transformed total plaque burden and 30y-FRS as covariates, respectively. The line in **A**, **C**, and **E** represents the regression line and the shading around it corresponds to the 95% confidence interval. Color bars in **B**, **D**, and **F** represent the magnitude of the voxel significance corrected for multiple comparisons ($P_{FWE\text{-}corr}$). L = left; R = right; other abbreviations as in Figures 1 and 2.

profile is associated with global brain hypometabolism; 2) this association is mainly driven by the presence of hypertension; 3) carotid atherosclerotic plaque burden is associated with global brain hypometabolism even after adjustment for CVD risk; and 4) hypometabolic brain regions associated with CVD risk and subclinical atherosclerosis in midlife include areas known to be affected in dementia (**Central Illustration**). To the best of our knowledge, this is the first study showing an association between hypometabolism in dementia-relevant brain regions, especially of the AD type, with CVD risk and atherosclerosis in a cohort of young asymptomatic individuals. These data are of the highest relevance because they suggest that strategies for early intervention may contribute to the prevention of dementia, decreasing its burden.

The association between CVRFs and cognitive decline is well established (8,29-31). A high FRS is linked to a faster decline in the perceptual speed and episodic and working memory of cognitively unimpaired older adults (32). Interestingly, intensive blood pressure control (33) and ideal cardiovascular health during midlife (34) have been linked to a reduced risk of dementia later in life. Indeed, stroke and dementia share common modifiable risk factors (35), and lifestyle intervention strategies have a beneficial effect on cognition (36), further suggesting that CVRFs may be causally associated with the development of dementia, at least partially. The prevailing notion has been that cognitive decline is a late effect of long-term CVRF exposure. However, our study shows that the presence of CVRFs is associated with brain hypometabolism long before clinical symptoms are

CENTRAL ILLUSTRATION **High 30-Year Framingham Risk Score, the Presence of Hypertension, and the Atherosclerotic Burden in the Carotid Arteries Are Associated With Decreased Brain Metabolism in Middle-Aged Asymptomatic Individuals**

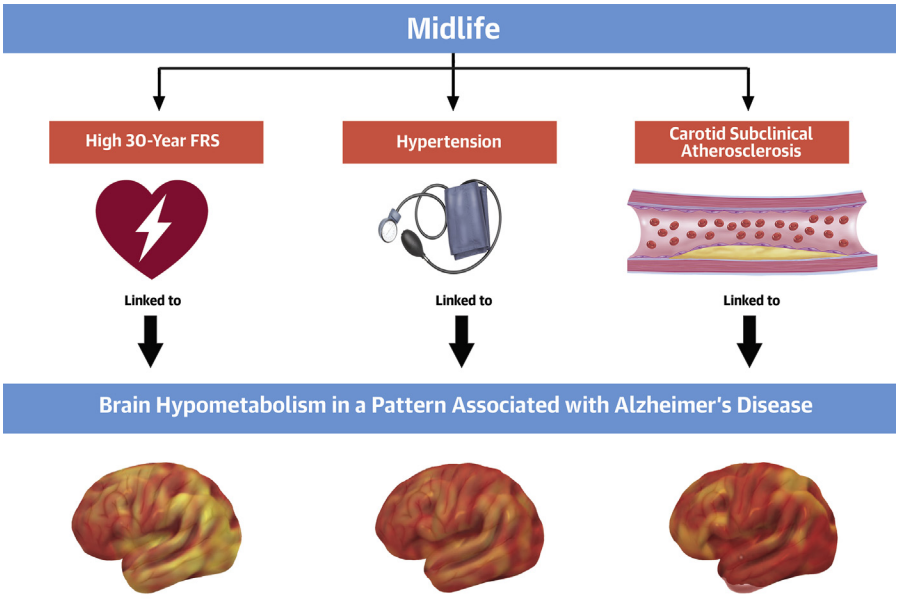

Cortes-Canteli, M. et al. J Am Coll Cardiol. 2021;77(7):888–98.

PESA (Progression of Early Subclinical Atherosclerosis) participants with evidence of subclinical atherosclerosis underwent ^{18}F-fluorodeoxyglucose (FDG)-positron emission tomography (n = 547, 50 ± 4 years, 82% men). Cerebral FDG uptake showed an inverse correlation with 30-year Framingham Risk Score (FRS), with the presence of hypertension, and with carotid plaque burden, even after adjusting for 30-year FRS. The brain areas most strongly affected by hypometabolism were dementia-relevant brain regions, especially of the Alzheimer's disease type, such as parietotemporal areas (angular, supramarginal, and temporal gyri) and the cingulate gyrus. The color in the tridimensional brain images represents the actual magnitude of the association, with **yellow areas** indicating the lowest p values.

present. Remarkably, this hypometabolism is present in parietotemporal areas critical for spatial and semantic memory, language and visual processing, and learning and memory retrieval; most of these regions form part of a specific hypometabolic AD signature predictive of future cognitive deterioration (37-39). Therefore, in middle-aged individuals, hypometabolism in these brain areas may be interpreted as a marker of increased vulnerability to future cognitive decline due to AD (40). We also found that hypertension was the modifiable CVRF with the strongest link to brain hypometabolism. This association had an effect size considered medium, representing 150% the effect size of age in this study ($\beta = -0.24$, $p < 0.001$ for a mean age of 50.3 ± 4.4 years, Supplemental Table 1), a factor widely and long known to impact glucose tolerance (41). Curiously, this hypometabolism was mainly present in the cingulate gyri, a limbic structure involved in response to emotion, decision making, and memory storage, among other important features of cognition. Preservation of this region's metabolism has been linked to sustained cognition in healthy adults older than 80 years and is part of the FDG-PET cognitive resilience signature (42). Our data suggest that brain metabolism may be affected from the earliest stages of exposure to CVRFs.

Atherosclerosis and dementia often co-occur at advanced stages of both processes (8,10-12,43), and the key to future clinical management is to move toward analyzing these pathological conditions much earlier in their evolution. A recent study linked the presence of carotid atherosclerosis in midlife to vascular dementia 20 years later (13). Our results show that brain changes associated with atherosclerosis are already happening during midlife. These changes include brain hypometabolism in areas of the limbic system and the parietal lobe, regions intimately involved in neurocognitive function and that form part of the hypometabolic signature of AD

(37,44). Interestingly, the association between carotid plaque burden and brain hypometabolism remained after correcting for 30-year FRS, suggesting that these outcomes (carotid plaque and brain hypometabolism) are not just epiphenomena associated with CVRFs but might be causally linked. Carotid stenosis is linked to increased cognitive decline (45) and the ongoing CREST (Carotid Revascularization and Medical Management for Asymptomatic Carotid Stenosis Study) trial will unravel whether this decline is reversible after revascularization (46). Although PESA study participants do not present carotid stenosis, we cannot discard that carotid plaque burden may be contributing to small changes in cerebral flow hemodynamics impacting brain metabolism. Also, although the ultrasound analysis in the PESA study only assesses extracranial carotid territories, it is plausible that intracranial segments were similarly diseased. Moreover, cerebral small vessel disease and other structural brain changes have been linked to midlife atherosclerosis (13), blood pressure variations (47), high FRS (32), other CVRFs (48), and even cognitive decline later in life (32,48). Our previous analysis of the PESA cohort revealed high interindividual differences in the vulnerability to atherosclerosis development, with some individuals with a high FRS not developing atherosclerosis, whereas others with a lower CVRF burden had extensive disease (21). Similarly, clinical CVD patients show interindividual differences in their vulnerability to dementia (9). Continued follow-up of our cohort will be key to understand whether midlife subclinical atherosclerosis may impact the brain's resilience to develop late-life cognitive deterioration.

The similar spatial pattern of brain hypometabolism to that seen in AD is intriguing. Brain metabolism is reduced in individuals with cerebrovascular deficiency (29) and early stages of neurodegeneration (49). Hence, midlife CVRFs and subclinical atherosclerosis might result in a more vulnerable and less resilient brain in the event of having to cope with the pathological burden associated with AD later in life. There is evidence linking CVRFs in midlife to the presence of amyloid-β plaques and tau tangles in the brain in late life (50), the key pathological hallmarks of AD (49). Interestingly, impaired amyloid-β clearance is a suggested link between atherosclerosis with AD (43), and amyloid-β accumulation (51) and tau deposition (52) are thought to start in areas matching the hypometabolic brain regions found in our analysis. Further research will be needed to define the precise mechanism linking CVRFs to the development of AD.

STUDY STRENGTHS AND LIMITATIONS. Our study has 2 main strengths. The first is the large population size; to our knowledge, no previous reports have analyzed such a large number of cerebral FDG-PET scans of asymptomatic middle-aged individuals. The second is that participants' subclinical atherosclerosis burden was extremely well characterized by 3D vascular ultrasound, which provides information on the plaque presence, number, and volume, giving precise information about individual vulnerability (25). Some limitations also need to be acknowledged. First, the lack of information about the cognitive status of the participants and the cross-sectional nature of our study limit the clinical implications because we cannot conclude at this moment that there is a cause-and-effect relationship between subclinical atherosclerosis, neurodegeneration (i.e., brain hypometabolism), and cognitive status. Despite not expecting significant clinical deterioration of our participants because of their young age, the longitudinal studies of this cohort, including cognitive measures, are warranted to provide information about the cues leading to the symptomatic stages of both disorders. In line with this, the consideration that brain hypometabolism is a predictor of cognitive decline or dementia, particularly in middle-aged individuals, should be interpreted with caution given the relatively small effect sizes observed in our study. Nevertheless, the important clinical significance of such small effect sizes in middle-aged asymptomatic participants is evidenced when compared with effect sizes (i.e., -0.54 ± 0.21) obtained when analyzing the well-established association between FDG uptake and cognitive function in elderly individuals with mild cognitive impairment (37). Second, given that an inclusion criterion to enter in this PET imaging study was the evidence of subclinical atherosclerosis, the generalization of the association between risk factors and brain hypometabolism should be done with caution for subjects without the former. In addition, our cohort is 100% Caucasian; thus, we cannot assume that these associations will be present in other races. Validation of our findings in other cohorts is thus required.

CONCLUSIONS

The findings presented here suggest that the interplay between CVRFs, atherosclerosis, and altered brain metabolism starts early in life. The potential ability of a modifiable disorder (CVD) to drive the evolution of a non-treatable condition (dementia) further supports

the critical value of implementing primary CVD prevention strategies early in midlife as a valuable therapeutic approach to delay or even stop downstream brain alterations, eventually leading to cognitive decline.

ACKNOWLEDGMENTS Special thanks to the PESA participants and the imaging, administrative, and medical PESA team at CNIC and at Banco Santander. The authors also thank Simon Bartlett for providing English editing.

FUNDING SUPPORT AND AUTHOR DISCLOSURES

The PESA study is co-funded equally by CNIC and Banco Santander, Madrid, Spain. The study also receives funding from the Instituto de Salud Carlos III, Madrid, Spain (ISCIII, PI15/02019), the European Regional Development Fund (ERDF-A Way to Build Europe) and the European Social Fund (ESF-Investing in Your Future). Dr. Cortes-Canteli was supported by a Miguel Servet type I research contract (ISCIII, CP16/00174 & MS16/00174) and the Fondo de Investigación Sanitaria (ISCIII, PI17/00590 & PI20/00819). Dr. Toribio-Fernandez was supported by the Iniciativa de Empleo Juvenil of the Consejería de Educación, Juventud y Deporte de la Comunidad de Madrid (PEJD-2018-POST/BMD-9259). Ms. Tristão-Pereira was supported by a "la Caixa" Foundation fellowship (ID 100010434, LCF/BQ/DI19/11730052). Dr. Gispert is supported by the Ministerio de Ciencia e Innovación (MCIN; RYC-2013-13054) and Dr. B. Ibanez by the European Research Council (ERC-2018-CoG 819775-MATRIX). The CNIC is supported by the ISCIII, the MCIN, and the Pro-CNIC Foundation. The BBRC is mainly funded by the "la Caixa" Foundation (ID 100010434) under agreement LCF/PR/GN17/50300004, the EU/EFPIA Innovative Medicines Initiative Joint Undertaking EPAD under grant agreement 115736, and the Innovative Medicines Initiative 2 Joint Undertaking under grant agreement 115952. This Joint Undertaking receives support from the European Union Horizon 2020 Research and Innovation Programme and the EFPIA. Dr. Molinuevo has served as a consultant for, sat on advisory boards of, or delivered lectures in symposia sponsored by Roche Diagnostics, Genentech, Novartis, Lundbeck, Oryzon, Biogen, Lilly, Janssen, Green Valley, MSD, Eisai, Alector, BioCross, GE Healthcare, and ProMIS Neurosciences. Dr. Gispert has given lectures in symposia sponsored by General Electric, Philips, and Biogen. Dr. Sanchez-Gonzalez is a Philips employee. All other authors have reported that they have no relationships relevant to the contents of this paper to disclose.

ADDRESS FOR CORRESPONDENCE: Dr. Valentin Fuster, Centro Nacional de Investigaciones Cardiovasculares, Melchor Fernández Almagro 3, 28029, Madrid, Spain. E-mail: vfuster@cnic.es. OR Dr. José Luis Molinuevo, Barcelonaβeta Brain Research Center, Alzheimer Prevention Program, C/ Wellington, 30, 08005 Barcelona, Spain. E-mail: jlmolinuevo@barcelonabeta.org. Twitter: @CNIC_CARDIO, @fpmaragall.

PERSPECTIVES

COMPETENCY IN MEDICAL KNOWLEDGE: Cardiovascular risk factors and subclinical carotid atherosclerosis in asymptomatic middle-aged people are associated with impaired cerebral metabolism in anatomic regions associated with cognitive decline later in life.

TRANSLATIONAL OUTLOOK: Additional research is needed to determine whether the associations between cardiovascular risk factors, subclinical atherosclerosis, and brain hypometabolism are causally related to subsequent cognitive decline and whether this can be translated into effective strategies to prevent dementia.

REFERENCES

1. Herrington W, Lacey B, Sherliker P, Armitage J, Lewington S. Epidemiology of atherosclerosis and the potential to reduce the global burden of atherothrombotic disease. Circ Res 2016;118:535–46.

2. Kristensen KE, Knage CC, Nyhegn LH, et al. Subclinical atherosclerosis is associated with incident atrial fibrillation: a systematic review and meta-analysis. Europace 2020;22:991–1000.

3. Planas-Ballvé A, Crespo AM, Aguilar LM, et al. The Barcelona-Asymptomatic Intracranial Atherosclerosis study: subclinical intracranial atherosclerosis as predictor of long-term vascular events. Atherosclerosis 2019;282:132–6.

4. Ahmadi A, Argulian E, Leipsic J, Newby DE, Narula J. From subclinical atherosclerosis to plaque progression and acute coronary events: JACC state-of-the-art review. J Am Coll Cardiol 2019;74:1608–17.

5. Mach F, Baigent C, Catapano AL, et al. 2019 ESC/EAS Guidelines for the management of dyslipidaemias: lipid modification to reduce cardiovascular risk. Eur Heart J 2020;41:111–88.

6. Piepoli MF, Hoes AW, Agewall S, et al. 2016 European guidelines on cardiovascular disease prevention in clinical practice: The Sixth Joint Task Force of the European Society of Cardiology and Other Societies on Cardiovascular Disease Prevention in Clinical Practice (constituted by representatives of 10 societies and by invited experts) Developed with the special contribution of the European Association for Cardiovascular Prevention & Rehabilitation (EACPR). Eur Heart J 2016;37:2315–81.

7. Livingston G, Sommerlad A, Orgeta V, et al. Dementia prevention, intervention, and care. Lancet 2017;390:2673–4.

8. Cortes-Canteli M, Iadecola C. Alzheimer's disease and vascular aging. J Am Coll Cardiol 2020;75:942–51.

9. Xie B, Shi X, Xing Y, Tang Y. Association between atherosclerosis and Alzheimer's disease: a systematic review and meta-analysis. Brain Behav 2020;10:e01601.

10. Dearborn JL, Zhang Y, Qiao Y, et al. Intracranial atherosclerosis and dementia: The Atherosclerosis Risk in Communities (ARIC) Study. Neurology 2017;88:1556–63.

11. Arvanitakis Z, Capuano AW, Leurgans SE, Bennett DA, Schneider JA. Relation of cerebral vessel disease to Alzheimer's disease dementia and cognitive function in elderly people: a cross-sectional study. Lancet Neurol 2016;15:934–43.

12. Hofman A, Ott A, Breteler MM, et al. Atherosclerosis, apolipoprotein E, and prevalence of dementia and Alzheimer's disease in the Rotterdam Study. Lancet 1997;349:151–4.

13. Gustavsson AM, van Westen D, Stomrud E, Engstrom G, Nagga K, Hansson O. Midlife atherosclerosis and development of alzheimer or vascular dementia. Ann Neurol 2020;87:52–62.

14. Baumgart M, Snyder HM, Carrillo MC, Fazio S, Kim H, Johns H. Summary of the evidence on modifiable risk factors for cognitive decline and dementia: a population-based perspective. Alzheimers Dement 2015;11:718–26.

15. Reiman EM, Chen K, Langbaum JBS, et al. Higher serum total cholesterol levels in late middle age are associated with glucose

hypometabolism in brain regions affected by Alzheimer's disease and normal aging. Neuroimage 2010;49:169–76.

16. Willette AA, Bendlin BB, Starks EJ, et al. Association of insulin resistance with cerebral glucose uptake in late middle-aged adults at risk for Alzheimer disease. JAMA Neurol 2015;72:1013–20.

17. Kuczynski B, Jagust W, Chui HC, Reed B. An inverse association of cardiovascular risk and frontal lobe glucose metabolism. Neurology 2009;72:738–43.

18. Toth PP. Subclinical atherosclerosis: what it is, what it means and what we can do about it. Int J Clin Pract 2008;62:1246–54.

19. Dubois B, Hampel H, Feldman HH, et al. Preclinical Alzheimer's disease: definition, natural history, and diagnostic criteria. Alzheimers Dement 2016;12:292–323.

20. Fernandez-Ortiz A, Jimenez-Borreguero LJ, Penalvo JL, et al. The Progression and Early detection of Subclinical Atherosclerosis (PESA) study: rationale and design. Am Heart J 2013;166:990–8.

21. Fernandez-Friera L, Penalvo JL, Fernandez-Ortiz A, et al. Prevalence, vascular distribution, and multiterritorial extent of subclinical atherosclerosis in a middle-aged cohort: the PESA (Progression of Early Subclinical Atherosclerosis) study. Circulation 2015;131:2104–13.

22. Fernandez-Friera L, Fuster V, Lopez-Melgar B, et al. Vascular inflammation in subclinical atherosclerosis detected by hybrid PET/MRI. J Am Coll Cardiol 2019;73:1371–82.

23. Pencina MJ, D'Agostino RB Sr., Larson MG, Massaro JM, Vasan RS. Predicting the 30-year risk of cardiovascular disease: the Framingham Heart study. Circulation 2009;119:3078–84.

24. Lopez-Melgar B, Fernandez-Friera L, Oliva B, et al. Subclinical atherosclerosis burden by 3D ultrasound in mid-life: the PESA study. J Am Coll Cardiol 2017;70:301–13.

25. Lopez-Melgar B, Fernandez-Friera L, Sanchez-Gonzalez J, et al. Accurate quantification of atherosclerotic plaque volume by 3D vascular ultrasound using the volumetric linear array method. Atherosclerosis 2016;248:230–7.

26. Gispert JD, Pascau J, Reig S, et al. Influence of the normalization template on the outcome of statistical parametric mapping of PET scans. Neuroimage 2003;19:601–12.

27. Rasmussen JM, Lakatos A, van Erp TG, et al. Empirical derivation of the reference region for computing diagnostic sensitive ^{18}fluorodeoxyglucose ratios in Alzheimer's disease based on the ADNI sample. Biochim Biophys Acta 2012;1822:457–66.

28. Spisák T, Spisák Z, Zunhammer M, et al. Probabilistic TFCE: a generalized combination of cluster size and voxel intensity to increase statistical power. Neuroimage 2019;185:12–26.

29. Sweeney MD, Montagne A, Sagare AP, et al. Vascular dysfunction-the disregarded partner of Alzheimer's disease. Alzheimers Dement 2019;15:158–67.

30. Iadecola C, Duering M, Hachinski V, et al. Vascular cognitive impairment and dementia: JACC Scientific Expert Panel. J Am Coll Cardiol 2019;73:3326–44.

31. Gottesman RF, Albert MS, Alonso A, et al. Associations between midlife vascular risk factors and 25-year incident dementia in the Atherosclerosis Risk in Communities (ARIC) Cohort. JAMA Neurol 2017;74:1246–54.

32. Song R, Xu H, Dintica CS, et al. Associations between cardiovascular risk, structural brain changes, and cognitive decline. J Am Coll Cardiol 2020;75:2525.

33. SPRINT MIND Investigators for the SPRINT Research Group, Williamson JD, Pajewski NM, et al. Effect of intensive vs standard blood pressure control on probable dementia: a randomized clinical trial. JAMA 2019;321:553–61.

34. Sabia S, Fayosse A, Dumurgier J, et al. Association of ideal cardiovascular health at age 50 with incidence of dementia: 25 year follow-up of Whitehall II cohort study. BMJ 2019;366:l4414.

35. Hachinski V, Einhaupl K, Ganten D, et al. Preventing dementia by preventing stroke: The Berlin Manifesto. Alzheimers Dement 2019;15:961–84.

36. Kivipelto M, Mangialasche F, Ngandu T. Lifestyle interventions to prevent cognitive impairment, dementia and Alzheimer disease. Nat Rev Neurol 2018;14:653–66.

37. Landau SM, Harvey D, Madison CM, et al. Associations between cognitive, functional, and FDG-PET measures of decline in AD and MCI. Neurobiol Aging 2011;32:1207–18.

38. Jagust W, Gitcho A, Sun F, Kuczynski B, Mungas D, Haan M. Brain imaging evidence of preclinical Alzheimer's disease in normal aging. Ann Neurol 2006;59:673–81.

39. Ewers M, Brendel M, Rizk-Jackson A, et al. Reduced FDG-PET brain metabolism and executive function predict clinical progression in elderly healthy subjects. Neuroimage Clin 2014;4:45–52.

40. Mosconi L, De Santi S, Li J, et al. Hippocampal hypometabolism predicts cognitive decline from normal aging. Neurobiol Aging 2008;29:676–92.

41. DeFronzo RA. Glucose intolerance and aging. Diabetes Care 1981;4:493–501.

42. Arenaza-Urquijo EM, Przybelski SA, Lesnick TL, et al. The metabolic brain signature of cognitive resilience in the 80+: beyond Alzheimer pathologies. Brain 2019;142:1134–47.

43. Gupta A, Iadecola C. Impaired Abeta clearance: a potential link between atherosclerosis and Alzheimer's disease. Front Aging Neurosci 2015;7:115.

44. Shivamurthy VK, Tahari AK, Marcus C, Subramaniam RM. Brain FDG PET and the diagnosis of dementia. AJR Am J Roentgenol 2015;204:W76–85.

45. Norling AM, Marshall RS, Pavol MA, et al. Is hemispheric hypoperfusion a treatable cause of cognitive impairment? Curr Cardiol Rep 2019;21:4.

46. Marshall RS, Lazar RM, Liebeskind DS, et al. Carotid revascularization and medical management for asymptomatic carotid stenosis - hemodynamics (CREST-H): study design and rationale. Int J Stroke 2018;13:985–91.

47. Ma Y, Yilmaz P, Bos D, et al. Blood pressure variation and subclinical brain disease. J Am Coll Cardiol 2020;75:2387.

48. Debette S, Seshadri S, Beiser A, et al. Midlife vascular risk factor exposure accelerates structural brain aging and cognitive decline. Neurology 2011;77:461.

49. Jack CR Jr., Bennett DA, Blennow K, et al. NIA-AA Research Framework: toward a biological definition of Alzheimer's disease. Alzheimers Dement 2018;14:535–62.

50. Petrovitch H, White LR, Izmirilian G, et al. Midlife blood pressure and neuritic plaques, neurofibrillary tangles, and brain weight at death: the HAAS. Honolulu-Asia aging Study. Neurobiol Aging 2000;21:57–62.

51. Palmqvist S, Scholl M, Strandberg O, et al. Earliest accumulation of beta-amyloid occurs within the default-mode network and concurrently affects brain connectivity. Nat Commun 2017;8:1214.

52. Cho H, Choi JY, Hwang MS, et al. In vivo cortical spreading pattern of tau and amyloid in the Alzheimer disease spectrum. Ann Neurol 2016;80:247–58.

KEY WORDS ^{18}F-fluorodeoxyglucose-positron emission tomography, Alzheimer's disease, cardiovascular risk, dementia, hypertension, statistical parametric mapping

APPENDIX For supplemental tables and figures, please see the online version of this paper.